https://doi.org/10.1016/j.energy.2017.10.124

Investigation on solar assisted liquid desiccant dehumidifier and evaporative cooling system for fresh air treatment

Yi Chen[a], Hongxing Yang[b,*], Yimo Luo[a]

[a]*Faculty of Science and Technology, Technological and Higher Education Institute of Hong Kong, Hong Kong*

[b]*Renewable Energy Research Group (RERG), Department of Building Services Engineering, The Hong Kong Polytechnic University, Hong Kong*

Abstract

The widely used semi-centralized air conditioning (A/C) system consisting of independent fresh air system and fan coil system suffers from huge energy consumption, especially for fresh air treatment. Therefore, a liquid desiccant dehumidifier and regenerative indirect evaporative cooling (LDD-RIEC) system is proposed for fresh air treatment. The fresh air is handled by the LDD-RIEC system in which no electricity-intensive compressor involves. The hot and humid fresh air is firstly dehumidified by LDD and then sensibly cooled by RIEC. The thermal energy captured by solar collectors is used for desiccant solution regeneration. Indoor return air is cooled by fan coils of a mechanical cooling system. The system performance is analyzed by solving the heat and mass transfer equations of each component integrally in a closed loop. Focus is placed on discussing the influences of solar collector area and inlet air conditions, and optimizing the extraction air ratio of RIEC. The energy saving ratio is quantitatively evaluated with respect to a conventional A/C system. Results reveal that the optimal extraction ratio is 0.3 considering the interacted influence of dehumidifier, regenerator, RIEC and solar collector. The energy saving ratio ranges from 22.4% to 53.2% under various inlet air conditions.

* Corresponding author.
E-mail address: hong-xing.yang@polyu.edu.hk (H. Yang)

Keywords: liquid desiccant dehumidifier; regenerative indirect evaporative cooling; system modeling; air-conditioning system; energy saving

1. Introduction

The semi-centralized air conditioning (A/C) system consists of independent fresh air system and fan coil system are more widely adopted in office buildings, hotels and some commercial buildings compared with all-air/centralized A/C system because of its simplicity, flexibility, economy and easy-controllability. The energy consumption for operating A/C system is huge, especially for treating the hot and humid fresh air [1]. It is reported that 20% to 40% of the overall building energy consumption is consumed by fresh air handling process [2]. Generally speaking, the lower the fresh air ratio, the smaller the total energy consumption. However, in recent decade, much more attention is being paid to the topics of improving indoor air quality (IAQ) since the large-scale outbreak of SARS virus and SBS (Sick Building Syndrome) in air-conditioned buildings [3]. Thus, there is contradictory between IAQ improvement by increasing fresh air ratio and energy conservation by reducing fresh air ratio. A high efficient fresh air handling scheme is urgently expected to balance the contradictory, in other words, to cool and dehumidify fresh air with less energy consumption.

The hybrid liquid desiccant dehumidification and regenerative indirect evaporative cooling system (LDD-RIEC) is therefore proposed as a promising energy-saving scheme for fresh air treatment in a semi-centralized A/C system. The hot and humid fresh air is firstly dehumidified by a LDD and then sensibly cooled by RIEC. In a LDD-RIEC system, there is no electricity-intensive compressor but only low-energy-consumed solution pumps and water pumps.

Therefore, the energy consumption of dehumidification and refrigeration is much less than a conventional Mechanical Vapor Compression Refrigeration (MVCR) system. The heat captured by solar collector is used for desiccant solution regeneration, which further improves the system's efficiency.

Under the trend of energy saving worldwide, the A/C system incorporated with dehumidification and evaporative cooling technology has drawn great research attentions in recent years [4~6]. Overall, the hybrid A/C system can be classified into solid desiccant-enhanced MVCR system [7~9], liquid desiccant-enhanced MVCR system [10] and hybrid desiccant + evaporative cooling system [11]. Solid desiccant is usually used in a desiccant wheel which is compact but has high pressure drop [12, 13]. Liquid desiccant has lower regeneration temperature and pressure drop but has corrosion problem [14]. Evaporative cooler (EC) can be classified into direct evaporative cooler (DEC) and indirect evaporative cooler (IEC) base on whether the primary air has contact with water. The IEC includes traditional plate type and tubular type cooler and advanced dew-point cooler [15]. The dew-point IEC, includes RIEC, M-cycle IEC and multi-stage IEC, is able to cool the primary air below the web-bulb temperature of inlet working air, and close to its dew point temperature.

The hybrid system, in its various aspects, has been intensively investigated theoretically and experimentally. The reported works are related to feasibility study, regional applicability study, performance prediction, parameter optimization and new material's development. The desiccant-enhanced MVCR system is proved to be superior to the conventional MVCR system in terms of energy saving and possibility of low-grade energy utilization [16]. The research shows that the system performs the best in high humid areas [17]. Among all hybrid A/C systems, the hybrid desiccant and evaporative cooling system seems to be the most promising one because it can handle both the sensible load and latent load without using MVCR system. La et al. [18] experimentally studied a novel rotary desiccant cooling system consisted of two-stage dehumidification and regenerative evaporative cooling. The system can produce 15–20°C high temperature chilled water and dry air at the same time. Enteria et al. [19] evaluated the desiccant-evaporative A/C system using the exergetic method. Percentage contributions of exergy destruction of system components at different regeneration temperatures and reference temperatures were determined. El Hourani et al. [20] optimized the design and operation of a 100% fresh air A/C system consisted by a solid desiccant dehumidification system and a two-stage evaporative cooling system. Regeneration temperature, air flow rate and air fraction entering the evaporative cooler are optimized with respect to energy and water consumption. Table 1 lists out some other representative studies related to the hybrid desiccant and evaporative cooling A/C system.

Table 1 Comparison of different types of hybrid desiccant and evaporative cooling A/C system

Ref.	System	Research contents
[21]	Plate type LDD + RIEC	Components model and experiment validation
[22]	Plate type LDD + M cycle IEC	Propose a simple and accurate approach for simulation the system, parameter analysis
[23]	Solar assisted LDD + IEC + DEC	Simulation based analysis (TRNSYS and commercial equation solver) for 100% fresh air
[24]	Solar assisted solid desiccant + IEC	Optimize the desiccant wheel supply/regeneration air ratio and IEC secondary/primary air ratio
[25]	LDD with solution recirculation + RIEC+DEC	Parametric study on solution self-cycle ratio, working to intake air ratio and regeneration temperature.
Present	Semi-centralized A/C system. Solar	Closed-cycle simulation; Analyze the

	assisted LDD + RIEC for fresh air and fan coils for return air	influences of solar collector area and inlet air conditions; Optimize extraction air ratio of RIEC and energy saving evaluation.

It can be seen that most existing studies related to modeling of hybrid liquid desiccant and evaporative cooling system are based on the multi-parameter fitting formula of components. Although accurate differential equation models have also been used in some studies, they were mainly open-loop based system simulation, which not consider the close-loop relationship of solution temperature and concentration between the dehumidifier and regenerator. In addition, in previously reported studies, only 100% fresh air A/C system or all-air A/C system was discussed, without much attention paid to the semi-centralized A/C system. Actually, the semi-centralized A/C system, which delivers cooling by both air and water, is much more widely used in hotels and office buildings with the high demand for flexibility and easy-controllability. Therefore, a LDD-RIEC semi-centralized A/C system is proposed. The fresh air treated by LDD-RIEC system can remove part of indoor cooling load. The rest of cooling load is handled by return air which is cooled by fan coils using chilled water from a MVCR system. Besides, the existing research on optimal extraction ratio of RIEC focuses on a stand-alone RIEC system [26]. The optimal extraction ratio in hybrid LDD-RIEC system considering the interacted influence of dehumidifier, regenerator, RIEC and solar collector has received few research attentions.

In this paper, the solar assisted LDD-RIEC semi-centralized A/C system is studied. Firstly, the working principles of the solar assisted LDD-RIEC semi-centralized A/C system is reported. Then, the development of the system model is presented by detailing the sub-models of each component. By using the validated model, a typical air handling process can be illustrated in the Psychrometric chart. The extraction air ratio of RIEC is optimized and the influences of solar collector area and inlet air conditions on system performance are analyzed. Finally, the energy saving ratio is quantitatively evaluated with respect to a conventional MVCR system under various operating conditions.

Nomenclatures

A	heat transfer area/solar collector area, m^2	h_m	mass transfer coefficient, $kg/m^2 \cdot s$
C	cooling capacity, W	h_{fg}	latent heat of vaporization of water, J/kg
I	solar radiation, W/m^2	i	enthalpy of air, J/kg
Q	heat transfer rate/cooling load, W	k	global heat transfer coefficient, $W/m^2 \cdot ℃$
V	air flow rate, m^3/h	m	mass flow rate, kg/s
W	electric power consumption, W	r_1	fresh air to total supply air ratio
c_{pa}	specific heat of air, J/kg·℃	r_2	extraction air ratio of RIEC
c_{pw}	specific heat of water, J/kg·℃	s	channel gap, m
c_{pso}	specific heat of solution, J/kg·℃	t	celsius temperature, ℃
d_e	hydraulic diameter, m	u	air velocity, m/s
h	heat transfer coefficient, $W/m^2 \cdot ℃$	xs	mass fraction of desiccant solution

Greek symbols

ω	moisture content of air, kg/kg	λ	thermal conductivity, W/m·℃
η	efficiency		

Subscripts

f	fresh/ primary air	lat	latent heat
r	return air	sen	sensible heat
s	secondary air	sat	saturated
w	wall/water	sup	supply air
ew	evaporation water	ct	cooling tower
in	inlet	D	dehumidifier
out	outlet	E	evaporative cooler
so	desiccant solution	R	regenerator
sc	solar collector	N	Indoor setting air condition
wb	wet-bulb		

Abbreviation

A/C	air-conditioning	RIEC	regenerative indirect evaporative cooler
RH	relative humidity	COP	coefficient of performance
IEC	indirect evaporative cooler/cooling	LDD	liquid desiccant dehumidifier
DEC	direct evaporative cooler/cooling	FCU	fan coil unit
SHR	Sensible heat ratio	LiCl	lithium chloride
MVCR	mechanical vapor compression refrigeration system		

2. LDD-RIEC semi-centralized air-conditioning system

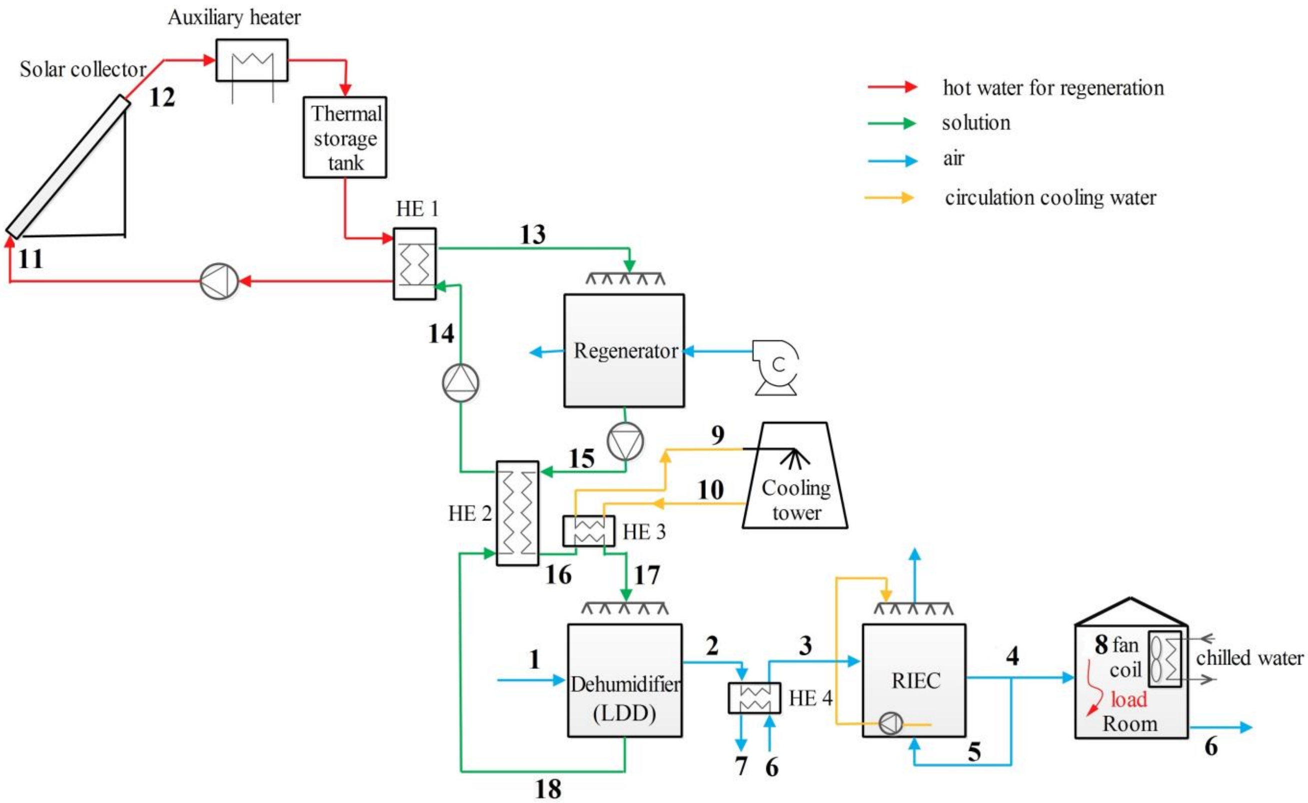

1	Inlet air of dehumidifier	$t_{f,D,in}$, $\omega_{f,D,in}$	10	Outlet water of cooling tower	$t_{w,ct,out}$
2	Outlet air of dehumidifier	$t_{f,D,out}$, $\omega_{f,D,out}$	11	Inlet water of solar collector	$t_{w,sc,in}$
3	Inlet air of RIEC	$t_{f,E,in}$, $\omega_{f,E,in}$	12	outlet water of solar collector	$t_{w,sc,out}$
4	outlet air of RIEC	$t_{f,E,out}$, $\omega_{f,E,out}$	13	Inlet solution of regenerator	$t_{so,R,in}$
5	secondary air of RIEC	$t_{s,E,in}$, $\omega_{s,E,in}$	14	Inlet solution of HE1	$t_{so,HE1,in}$
6	Indoor exhaust air supplied to HE4	$t_{ex,in}$	15	Outlet solution of regenerator	$t_{so,R,out}$
7	Outlet air of HE4	$t_{ex,out}$	16	Inlet solution of HE3	$t_{so,HE3,in}$
8	Supply air by fan coil	$t_{coil,out}$, $\omega_{coil,out}$	17	Inlet solution of dehumidifier	$t_{so,D,in}$
9	Inlet water of cooling tower	$t_{w,ct,in}$	18	Outlet solution of dehumidifier	$t_{so,D,out}$

Fig.1 System diagram of LDD-RIEC semi-centralized A/C system

Fig.1 shows the system diagram of a LDD-RIEC semi-centralized A/C system. It consists of an independent solar-assisted LDD-RIEC system for fresh air treatment and a fan coil unit (FCU) for return air treatment. The RIEC is used in the proposed system because of its much higher cooling efficiency compared with traditional IEC although a part of air is sacrificed as secondary air [27]. Besides, the price for producing additional dehumidified air is low because the driven heat is ‘free’ solar energy. Totally, there are 6 main components, including the solar collector, dehumidifier, regenerator, cooling tower, RIEC and fan coil. The heat captured by the solar collector is used for desiccant solution regeneration through a water/solution heat exchanger (HE1). Auxiliary heater would operate in case of thermal energy is insufficient for regeneration. Storage tank is used for storing excess heat. As high inlet solution temperature results in low dehumidification efficiency, a cooling tower is used for cooling the desiccant solution through a solution/water heat exchanger (HE3). The hot outlet air of dehumidifier is pre-cooled by the exhaust air from A/C room through an air/air heat exchanger (HE4) before sensibly cooled by RIEC. The indoor return air is handled by the FCU system. The FCU is assembled by a fan and a heat exchanger where the chilled water from a mechanical cooling unit is used as cooling media. The indoor return air is inhaled to FCU, cooled and dehumidified locally and then supplied to indoor. Overall, there are four loops in the LDD-RIEC semi-centralized A/C system, including hot water loop of solar collector, solution loop of dehumidifier and regenerator, cooling water loop and fresh air loop. The former three are closed loops and the last one is an open loop.

The detailed configuration of LDD-RIEC system is shown as Fig.2. The reversed moist air flow is dehumidified by the falling lithium chloride (LiCl) desiccant solution film in the LDD and then sensibly cooled by water evaporation in RIEC. The desiccant solution is sprayed into the dehumidifier, absorbs the water in the air and then pumped to the regenerator for regeneration by thermal energy. RIEC is an advanced IEC that has improved cooling efficiency compared with the traditional one by regenerating a part of produced air. The RIEC is consisted of a series of thin parallel plates assembled to form multi-layer alternating dry and wet channels. The water drop sprayed into the wet channels and cools the plate surface with the aid of water film evaporation. The fresh air in the dry channel is sensibly cooled by the cold plate. The 'regenerative' means that the wet channel extracts a part of produced air from the outlet of dry channel to form a secondary air flow in the wet channel [28, 29].

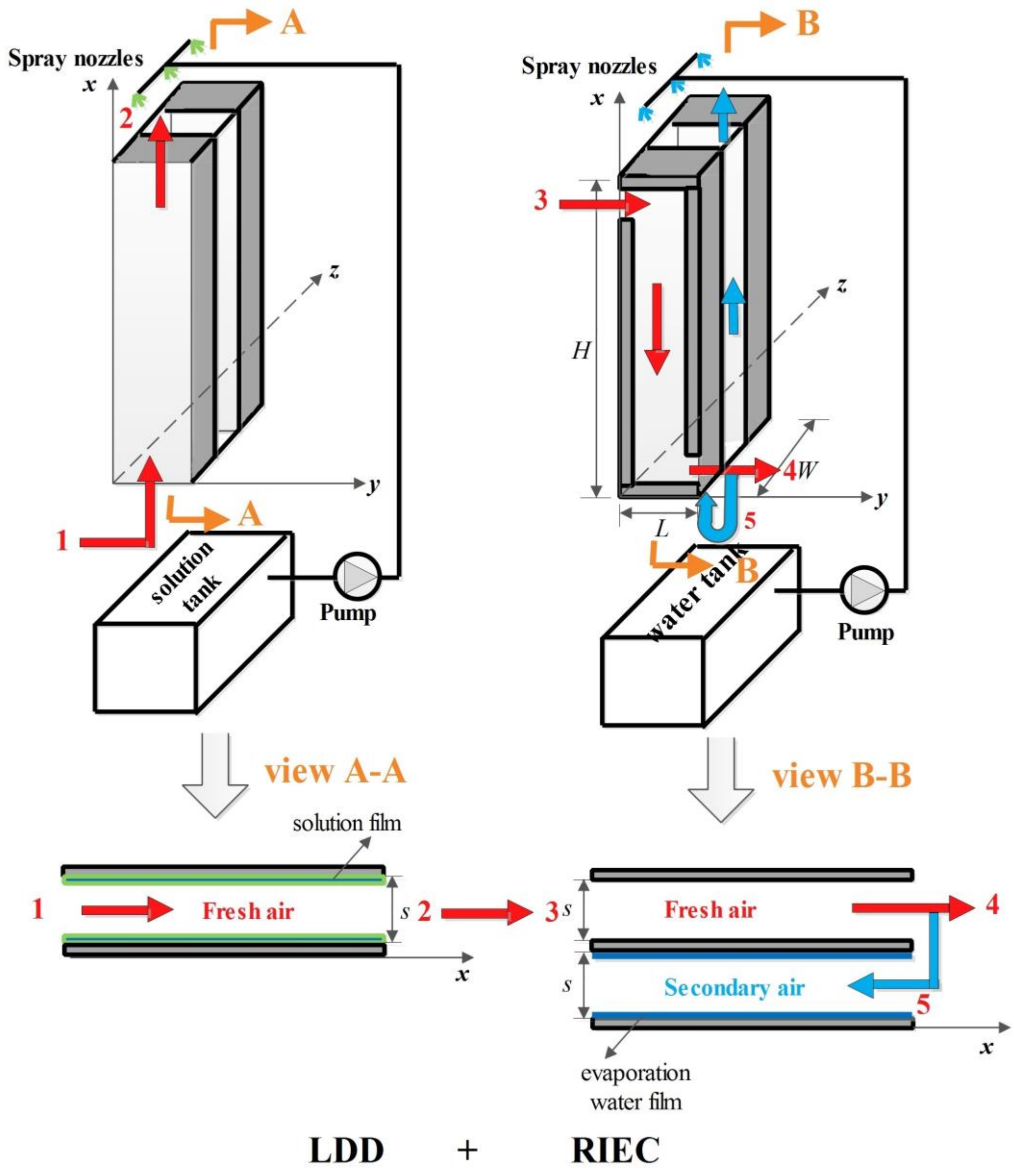

Fig.2 Detailed configuration of LDD-RIEC system

3. Model and validation

Each component model was established as follows to facilitate the system simulation.

3.1 Model of dehumidifier/regenerator

Adiabatic plate-type dehumidifier and regenerator with counter-flow configuration were used in this study. Several assumptions were made to simplify the complexity of the heat and mass transfer process: (1) properties of gas and liquid are constant; (2) heat and mass are only transferred vertically across the wall; (3) non-uniformity of air flow and solution flow is negligible; (4) thermal resistance of liquid film is negligible; (5) air-liquid interface temperature is equal to the bulk liquid temperature. Based on the assumptions, a one-dimensional finite difference model was employed for dehumidifier/regenerator analysis. The grid independency of the model has been checked with different mesh sizes from 5 to 200. The optimal number of domain elements was determined to be 100 by increasing elements until the outlet air temperature and humidity remain steady. For each microelement, the heat and mass transfer process follows the energy and mass conservation equations, listed as follows:

1) Mass conservation equation

$$m_{f,D} d\omega_f + dm_{\mathrm{so}} = 0 \tag{1}$$

2) Energy conservation equation

$$m_{f,D} di_f + d(i_{\mathrm{so}} m_{\mathrm{so}}) = 0 \tag{2}$$

3) Sensible heat exchange equation

$$m_{f,D} c_{\mathrm{pa}} dt_f = h_f (t_{\mathrm{so}} - t_f) dA \tag{3}$$

4) Overall heat exchange equation

$$m_{f,D} di_f = h_{mf}[(i_{\text{sat}} - i_f) - (1 - \frac{h_f}{h_{mf} c_{\text{pa}}}) c_{\text{pa}} (t_{\text{so}} - t_f)] dA \tag{4}$$

In this work, the local heat transfer coefficient is used for simulation instead of an average Nusselt number. Local Nusselt number was calculated by the following equations recommended by Li and Yang [30]:

$$Nu_x = 0.332(\text{Re}_x)^{1/2} (\text{Pr})^{1/3} (\text{Re}_x < 5 \times 10^4) \tag{5}$$

$$Nu_x = 0.0292(\text{Re}_x)^{0.8} (\text{Pr})^{1/3} (5 \times 10^4 < \text{Re}_x \leq 3 \times 10^7) \tag{6}$$

The local mass transfer coefficient is determined by Chilton-Colburn analogy. The specific thermal capacity of LiCl solution is the function of solution temperature and solution concentration, which was calculated according to the reference [31]. In addition, according to the mass balance of desiccant dehumidification and regeneration process, the air moisture loss in the dehumidifier equals to that gained in the regenerator.

$$m_{f,D} \left(\omega_{f,D,in} - \omega_{f,D,out} \right) = m_{f,\text{R}} \left(\omega_{f,\text{R},out} - \omega_{f,\text{R},in} \right) \tag{7}$$

The energy-consumed components in the solar-assisted LDD system include solution pump, heating water pump and two fans, which can be calculated as follows.

$$W_{fan} = \frac{V \times \Delta P}{3600 \times 1000 \times \eta_0 \times \eta_1} \times K \tag{8}$$

$$W_{pump} = m_w \cdot g \cdot H \cdot K \tag{9}$$

where, ΔP is pressure drop, pa; H is the head of the pump, m; η_0 is the internal efficiency of the fan, ranging from 0.7~0.8; η_1 is the mechanical efficiency which determined by the connection method between the motor and fan, ranging from 0.95~1.0; and K is motor capacity coefficient. In this study, η_0, η_1 and K are assumed as 0.75, 0.95 and 1.15, respectively.

3.2 Model of RIEC

The model of RIEC is established based on the energy and mass balance in the two channels by adopting the same assumptions as made in the dehumidifier. The one-dimensional finite difference method was also employed for RIEC analysis.

1) Heat balance of secondary air

$$h_s(t_w - t_s)dA = c_{pa} m_{s,E} dt_s \tag{10}$$

2) Mass balance of secondary air

$$h_{ms}(\omega_{sat} - \omega_s)dA = m_{s,E} d\omega_s \tag{11}$$

3) Heat balance of primary air

$$h_f(t_f - t_w)dA = c_{pa} m_{f,\mathrm{E}} dt_f \tag{12}$$

4) Mass balance of evaporation water film

$$dm_{ew} = m_s d\omega_s \tag{13}$$

5) Overall energy balance equation

$$m_s di_s - c_{pa} m_{f,E} dt_f = d(c_{pw} t_{ew} m_{ew}) \tag{14}$$

The mass flow rates of primary air and secondary air satisfy the relationship:

$$m_s = r_2 \cdot m_{f,E} \tag{15}$$

The relationship between the supply airflow rate to the room (m_{sup}), primary air flow rate of RIEC ($m_{f,E}$) and fresh air flow rate of LDD ($m_{f,D}$) can be expressed as follows considering additional air (r_2) redirected to secondary channels. The m_{sup} is decided upon the fresh air demand.

$$m_{f,D} = m_{f,\mathrm{E}} = \frac{m_{\mathrm{sup}}}{1 - r_2} \tag{16}$$

The equation for calculating the heat transfer coefficient of fully-developed laminar flow is [32, 33]:

$$Nu = \frac{h \cdot d_e}{\lambda} = 8.235 \tag{17}$$

The mass transfer coefficient (h_{ms}) can be obtained by assuming that the Lewis relationship is satisfied and Lewis number is unity in the air-water interacted surface. For RIEC, the boundary conditions are: x=H, t_f=$t_{f,E,in}$; x=0, $t_{s,in}$=$t_{f,E,out}$; x=0, $\omega_{s,E,in}$=$\omega_{f,E,in}$; x=H, m_{ew}=$m_{ew,in}$. The energy consumption of RIEC including the supply air fan, exhaust air fan and pump can be calculated by the correlations given in the reference [34].

3.3 Model of FCU

The FCU is used to cool the return air by chilled water from a MVCR system. However, the MVCR system in a LDD-RIEC A/C system is different from that in a traditional MVCR system in two aspects. Firstly, all or part of the latent load is removed by LDD and a part of the sensible load is handled by RIEC. Thus, the FCU are only responsible for the rest of cooling load. Secondly, the FCU can be operated at two possible conditions: dry-coil and wet-coil. For the former condition, all the latent load is handled by the treated fresh air and the FCU only needs to meet the rest of sensible load. Therefore, chilled water temperature is unnecessary to be very low without the need for dehumidification. The energy efficiency of the chiller can be greatly improved by increasing chilled water temperature. For the latter condition, the commonly used low temperature chilled water is still needed for removing the rest of latent load and sensible load. The cooling load of FCU can be calculated as:

$$Q_{coil} = Q_{load} - m_{\sup} h_{fg} \left(\omega_N - \omega_{f,D,out} \right) - m_{\sup} c_{pa} \left(t_N - t_{f,E,out} \right) \tag{18}$$

Where, Ql_{oad} is the total cooling load, kW; $m_{\mathrm{sup}} h_{fg} \left(\omega_N - \omega_{f,D,out} \right)$ is the latent load removed by LDD and $m_{\mathrm{sup}} c_{pa} \left(t_N - t_{f,E,out} \right)$ is the sensible load removed by RIEC.

Energy consumption of the chiller can be estimated by:

$$W_{chiller} = \frac{Q_{coil}}{COP} \tag{19}$$

From the literature, the average COP of conventional MVCR system is 3.3 simulated by Energyplus under the chilled water temperature of 7℃ and evaporation temperature of 2℃. However, the average COP increases to 4.62 when chilled water is 15℃ and evaporation temperature is 13℃ [35]. Thus, the COP of chiller under FCU wet-coil condition and dry-coil condition are 3.3 and 4.62, respectively.

3.4 Models of other components

Other components' models including cooling tower, heat exchanger and solar collector were established separately as follow. The efficiency of cooling tower can be defined as:

$$\eta_{ct} = \frac{t_{w,ct,in} - t_{w,ct,out}}{t_{w,ct,in} - t_{wb,f,in}} \tag{20}$$

Take HE3 as an example, the heat transfer rate between desiccant solution and cooling water can be calculated as:

$$Q_{ct} = m_{so} c_{pso} (t_{so,HE3,in} - t_{so,D,in}) \tag{21}$$

$$Q_{ct} = kA\Delta t = kA \frac{(t_{so,HE3,in} - t_{w,ct,in}) - (t_{so,D,in} - t_{w,ct,out})}{In(t_{so,HE3,in} - t_{w,ct,in}) / (t_{so,D,in} - t_{w,ct,out})} \tag{22}$$

The efficiency of evacuated tube solar collectors can be calculated as follows according to the test results from Hocschul Rapperswil of Switzerland [36].

$$\eta_{sc} = 0.84 - \frac{2.02(t_m - t_{amb})}{I} - 0.0046(\frac{t_m + t_{amb}}{2})^2 \tag{23}$$

The efficiency of solar collector is also defined as:

$$\eta_{sc} = \frac{Q_u}{A \cdot I} = \frac{\sigma A \cdot [\eta I - U_L(t_m - t_{amb})]}{A \cdot I} = \frac{m_w c_{pw}(t_{w,sc,out} - t_{w,sc,in})}{A \cdot I} \tag{24}$$

where, Q_u is the useful thermal energy collected for water heating; σ is the absorber area to gross area ratio; η is the absorber efficiency; U_L is the overall heat loss coefficient, W/m^2·℃; t_{amb} is the ambient air temperature and t_m is the mean water temperature in the solar collector, ℃. The value for each parameter is listed in Table 2.

3.5 Performance indicators

Five performance indicators, including sensible/latent cooling capacity of the LDD-RIEC system (C_{sen}/C_{lat}), sensible/latent load removed rate from an air-conditioned space (Q_{sen}/Q_{lat}) and overall COP of the A/C system, were used to evaluate the system's performance. They are calculated as Eq.(25) to Eq.(29), respectively.

$$C_{sen} = m_{\mathrm{sup}} c_{pa}(t_{f,D,in} - t_{f,\mathrm{E},out}) \tag{25}$$

$$C_{lat} = m_{\mathrm{sup}} h_{fg}(\omega_{f,D,in} - \omega_{f,\mathrm{D},out}) \tag{26}$$

$$Q_{sen} = m_{\mathrm{sup}} c_{pa}(t_N - t_{f,E,out}) \tag{27}$$

$$Q_{lat} = m_{\mathrm{sup}} h_{fg}(\omega_N - \omega_{f,\mathrm{D},out}) \tag{28}$$

$$COP = \frac{C_{sen} + C_{lat} + Q_{coil}}{W_{LDD} + W_{RIEC} + W_{coil}} \tag{29}$$

3.6 Model validation

Considering the routine models of other components are mature, validation was only conducted for the LDD and RIEC. Firstly, the RIEC model was validated by comparing the numerical simulation results with those experimental data obtained from a counter-flow RIEC [37]. The simulations were conducted by setting the same flow pattern, unit geometry and inlet air conditions as given in the literature. Comparisons between simulation results and the experimental results are shown in Fig.3. Small discrepancies can be found under various inlet air temperature and humidity.

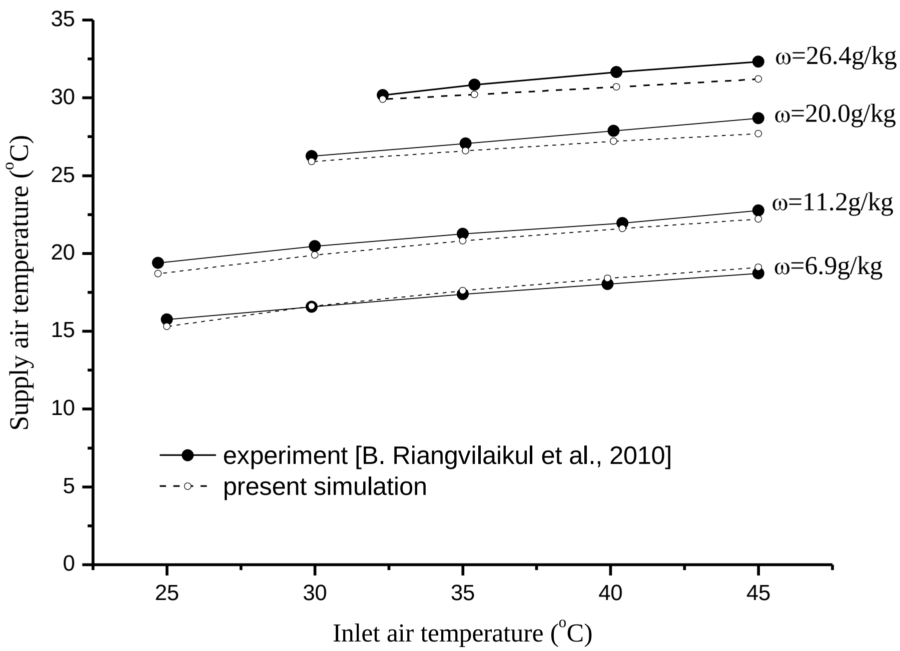

Fig.3 Comparison of RIEC simulation results with experimental results

Secondly, the LDD model was validated using the experimental data obtained from a packed LDD tower [38]. The simulated outlet moisture difference agrees well with the experimental data under various cases, as shown in Fig.4. Consequently, components' models are reliable for analyzing the performances of the whole system..

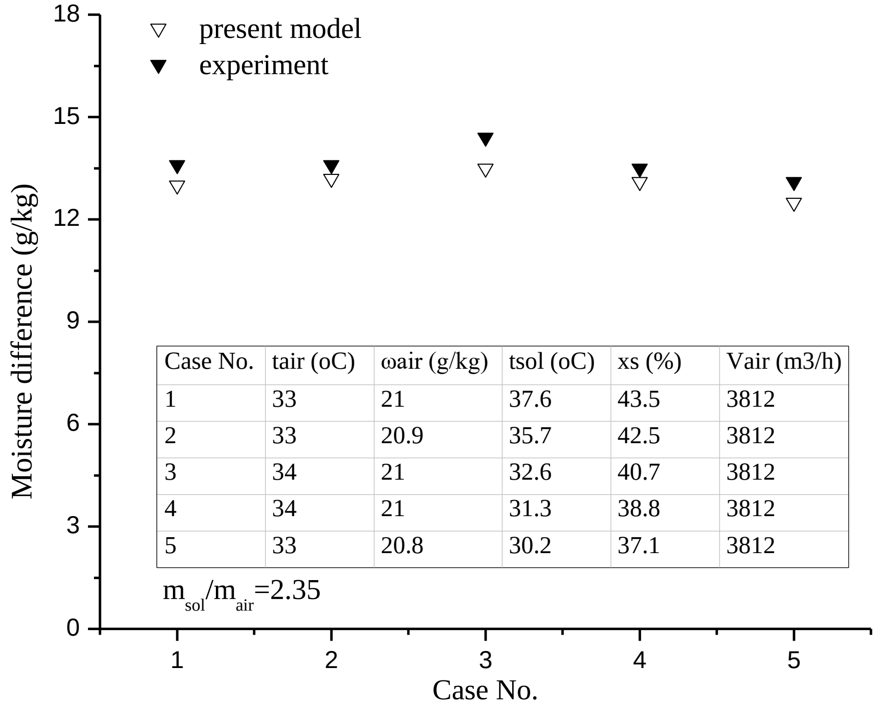

Case No.	tair (oC)	ωair (g/kg)	tsol (oC)	xs (%)	Vair (m3/h)
1	33	21	37.6	43.5	3812
2	33	20.9	35.7	42.5	3812
3	34	21	32.6	40.7	3812
4	34	21	31.3	38.8	3812
5	33	20.8	30.2	37.1	3812

Fig.4 Comparison of LDD simulation results with experimental results

3.7 Simulation procedure of the LDD-RIEC semi-centralized A/C system

Totally, the LDD-RIEC semi-centralized A/C system model consists of ten components' models (solar collector, dehumidifier, regenerator, cooling tower, RIEC, FCU, HE1, HE2, HE3 and HE4), with three (dehumidifier, regenerator and RIEC) being first-order ordinary differential equations. The differential equations were solved using the Runge-Kutta approach.

Before simulation, geometrical parameters of each component and weather data were input to the model. The simulation started from the solar collector. The total heat captured by the solar collector was set as the input to HE1. Initial values were required as a starting point for the closed-loop simulation of dehumidifier and regenerator. The closed-loop simulation started from the initial values of inlet solution concentration (*xs*) and temperature of the dehumidifier ($t_{so,D,in}$), which were then updated by the sub-models of heat exchangers, cooling tower, regenerator and overall moisture balance. Once all the mass and energy balance equations were satisfied, the final operating values of solution concertation, solution temperature, outlet air temperature and humidity can be obtained. The detailed closed-loop simulation flow chart for the solar assisted dehumidifier and regenerator cycle is shown in Fig.5.

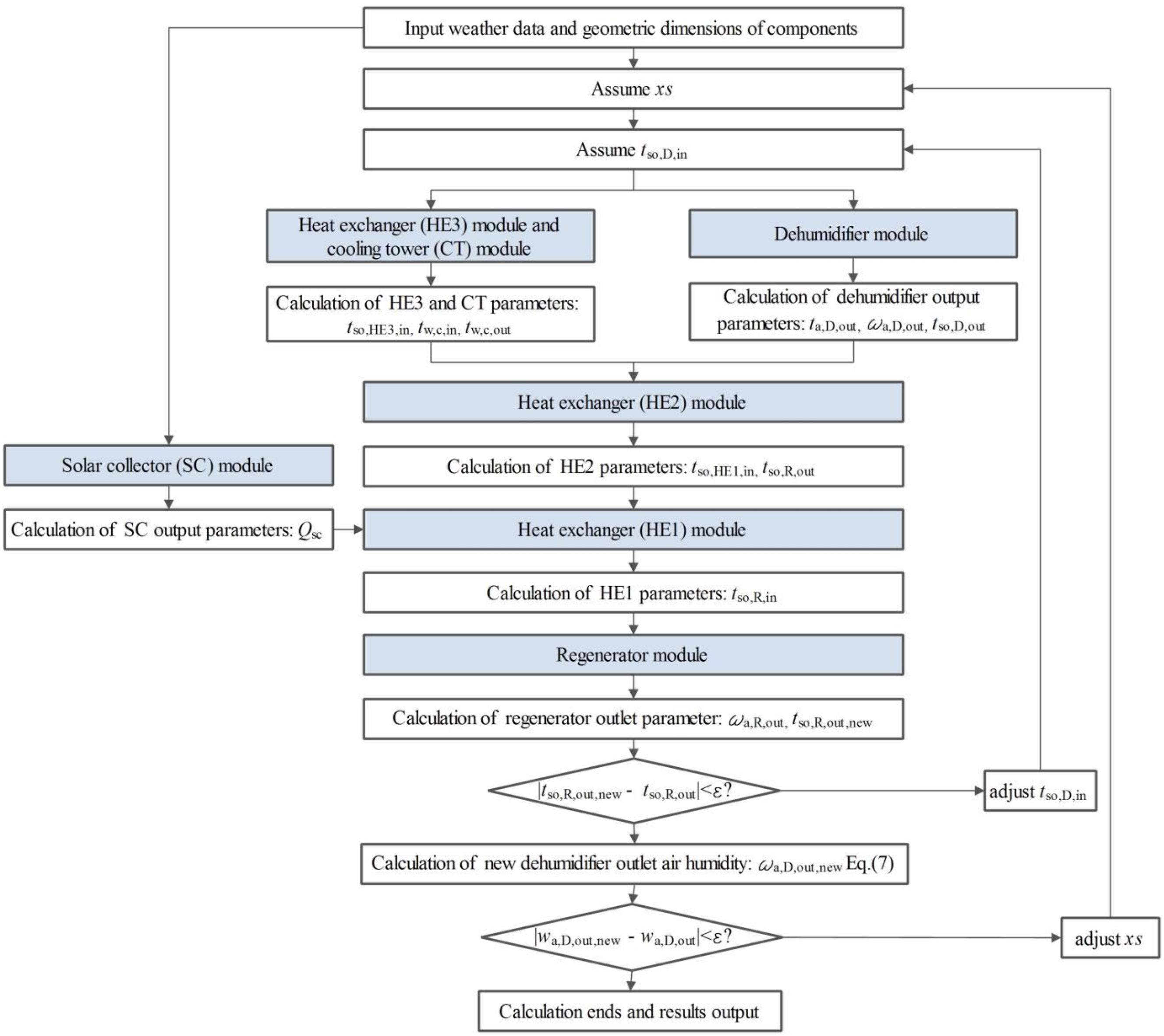

Fig.5 Simulation flow chart of the dehumidifier and regenerator as a closed-loop

With availability of the outlet air temperature and humidity from LDD, the inlet air conditions of RIEC were known. The outlet air parameters of RIEC can be obtained using the RIEC model by inputting its geometrical parameters and inlet air parameters. The parameters of each component used in the simulation are summarized in Table 2. The solar collector area is determined by the sensitivity analysis in section 4.3. It is determined to be 50 m^2 to ensure the best thermal performance of the LDD-RIEC system under given air conditions (30℃, 20g/kg). The value of extraction ratio (r_2) of RIEC is determined by the optimization result in section 4.2. The values of other simulation parameters are based on the empirical values from references.

Table 2 Simulation parameters of system components

Component	Parameter	Value
Solar collector	Solar collector gross area	50m^2
	Absorber area to gross area ratio	0.7
	Absorber efficiency	0.96
	Solar radiation	400W/m^2
	Total thermal loss coefficient	1.2W/ m^2·℃
	Heating water flow rate	0.2kg/s
Auxiliary heater	Efficiency	0.9
Dehumidifier/Regenerator	NTU	2.0
	Desiccant flow rate	0.2kg/s
	Air flow rate	0.1kg/s
	Inlet air temperature and humidity	30℃, 20g/kg
Cooling tower	Efficiency	0.46
	Cooling water flow rate	0.2kg/s
RIEC	Channel pairs	25
	Height × width	1.0m×0.5m
	Channel gap	4mm
	Air flow rate	0.1kg/s
	Extraction ratio (r_2)	0.3
Heat exchanger	Efficiency	HE1: 0.9; HE4: 0.65
	Heat transfer area	HE2: 2m^2, 800W/m^2·℃
	Total heat transfer coefficient	HE3: 1m^2, 800W/m^2·℃
FCU	Chiller COP	4.62 (dry-coil) 3.3 (wet-coil)

4. Results and discussion

4.1 Air handling process

As previously mentioned, the FCU could be operated under dry-coil and wet-coil conditions. In this section, an example of air handling process of LDD-RIEC semi-centralized A/C system under FCU dry-coil condition is illustrated in a Psychrometric chart. The total sensible load is set to be 1239W and total latent load is 585W. As shown in Fig.6. The fresh air (30℃, 20g/kg) is firstly dehumidified by the LDD, then pre-cooled by HE4 and finally supplied to RIEC. In the RIEC, 30% of the outlet air in the dry channel is extracted to form as secondary air in the wet channel. The fresh air supplied to RIEC can be cooled from 33.3℃ to 17.4℃ without humidity change and the humidified secondary air is exhausted. The fresh air treated by the LDD-RIEC system is designed to remove all the latent load of fresh air and internal gains. Thus, the FCU can operate at dry-coil condition using 15℃ chilled water as cooling media. The indoor return air is sensibly cooled from 26℃ to 17℃ and mixed with the treated fresh air, finally providing cool and dry supply air of 17.2℃ and 9.8g/kg.

In this case, all latent load and 606W sensible load are removed by supplied fresh air. The rest 633W sensible load is handled by FCU. Based on the methods in Section 3.1 to Section 3.3, the breakdown of major parasitic electrical power consumptions in the LDD-RIEC system is listed in Table 3. The energy consumption of FCU for treating return air is estimated to be 137W. In all, the energy consumption of LDD-RIEC semi-centralized A/C system is 296W.

Table 3 Breakdown of major electrical power consumptions

Solar collector	LDD			RIEC	
Pump (W)	Pumps (W)	Fan (W)	Cooling tower (W)	Pump (W)	Fan (W)
54	22	28	22	11	22

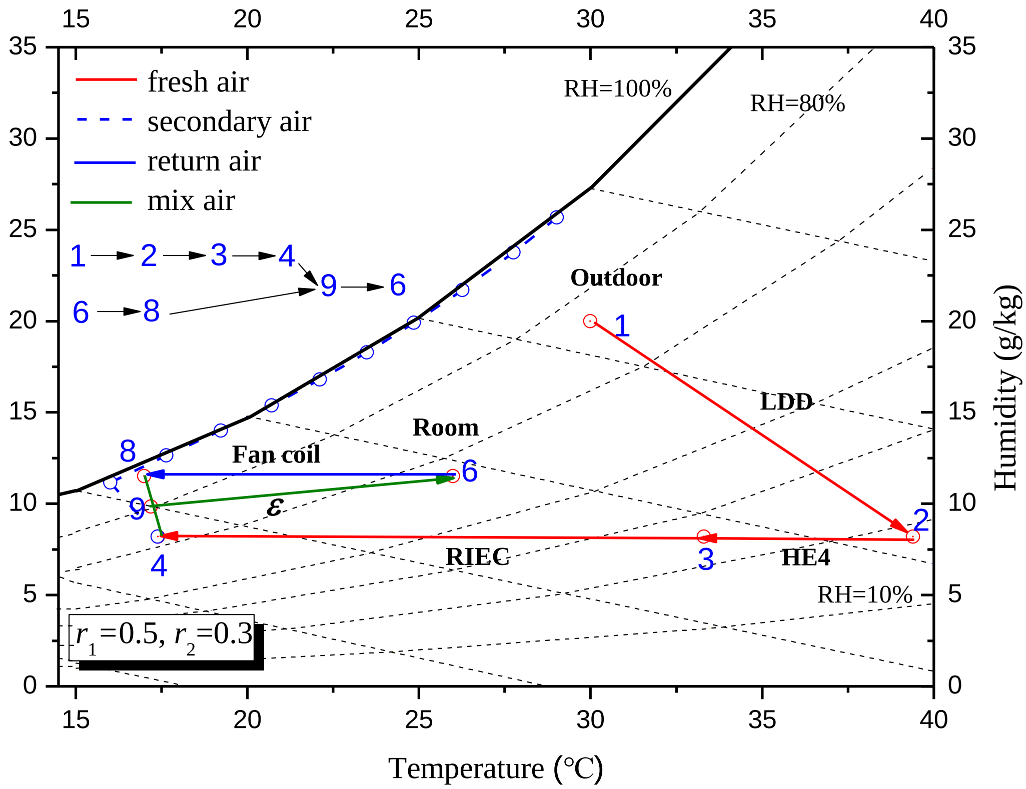

Fig.6 Psychrometric chart illustrated air handling process of LDD-RIEC semi-centralized A/C system

To compare the energy consumption of a conventional MVCR system with the proposed system, equivalent cooling load in the above case is eliminated by a MVCR system. The psychrometric chart illustrated air handling process of MVCR A/C system is shown in Fig.7. The fresh air and indoor return air are firstly mixed before centralized treated by the fan coils. Because of the simultaneous need for cooling and dehumidification, the FCU needs to operate under wet-coil condition using 7℃ chilled water. The outlet mixed air from FCU is

17℃ and 9.8g/kg. Under the giving case, the energy consumption for treating the mixed air is estimated to be 553W. Thus, 46% of the electricity saving is achieved by adopting LDD-RIEC system owing to the low-energy-consumed fresh air treatment approach.

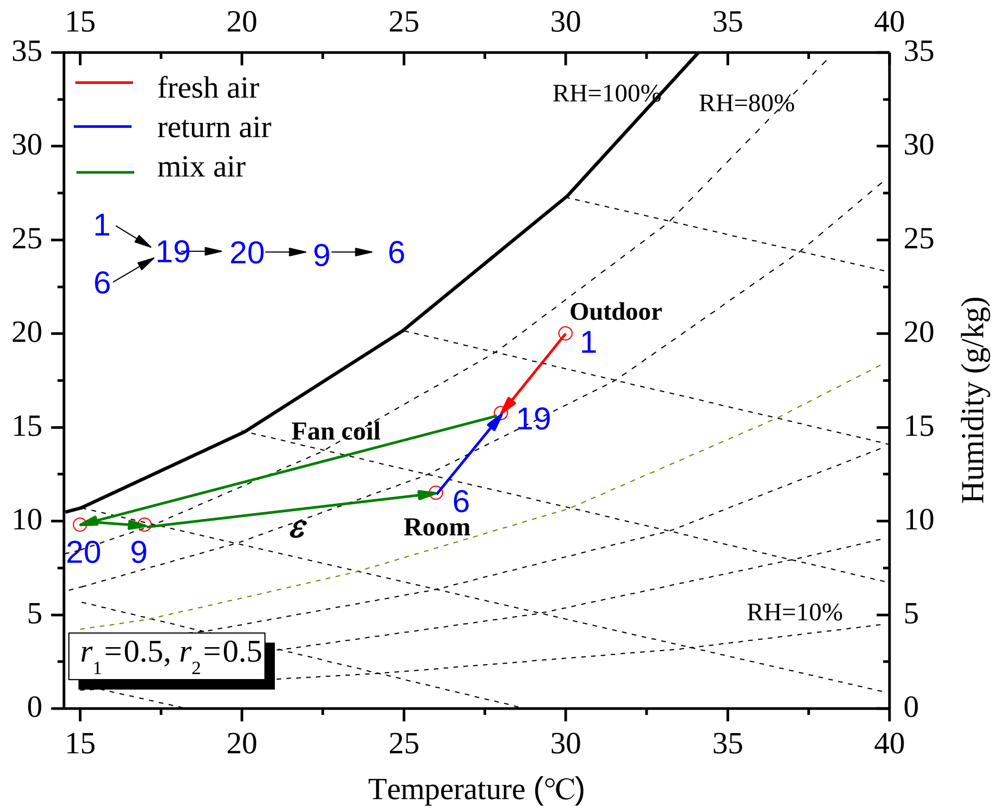

Fig.7 Psychrometric chart illustrated air handling process of MVCR A/C system

4.2 Extraction air ratio optimization

In a RIEC, the wet channel extracts a part of fresh air from the outlet of dry channel to form a secondary air flow in the wet channel. The extraction ratio defined as the secondary air flow rate to total air flow rate greatly affect the RIEC cooling performance. Larger extraction ratio can help improve the cooling efficiency but more produced air will be sacrificed to work as secondary air. Therefore, it is important to optimize the extraction ratio in terms of the whole solar-assisted LDD-RIEC system.

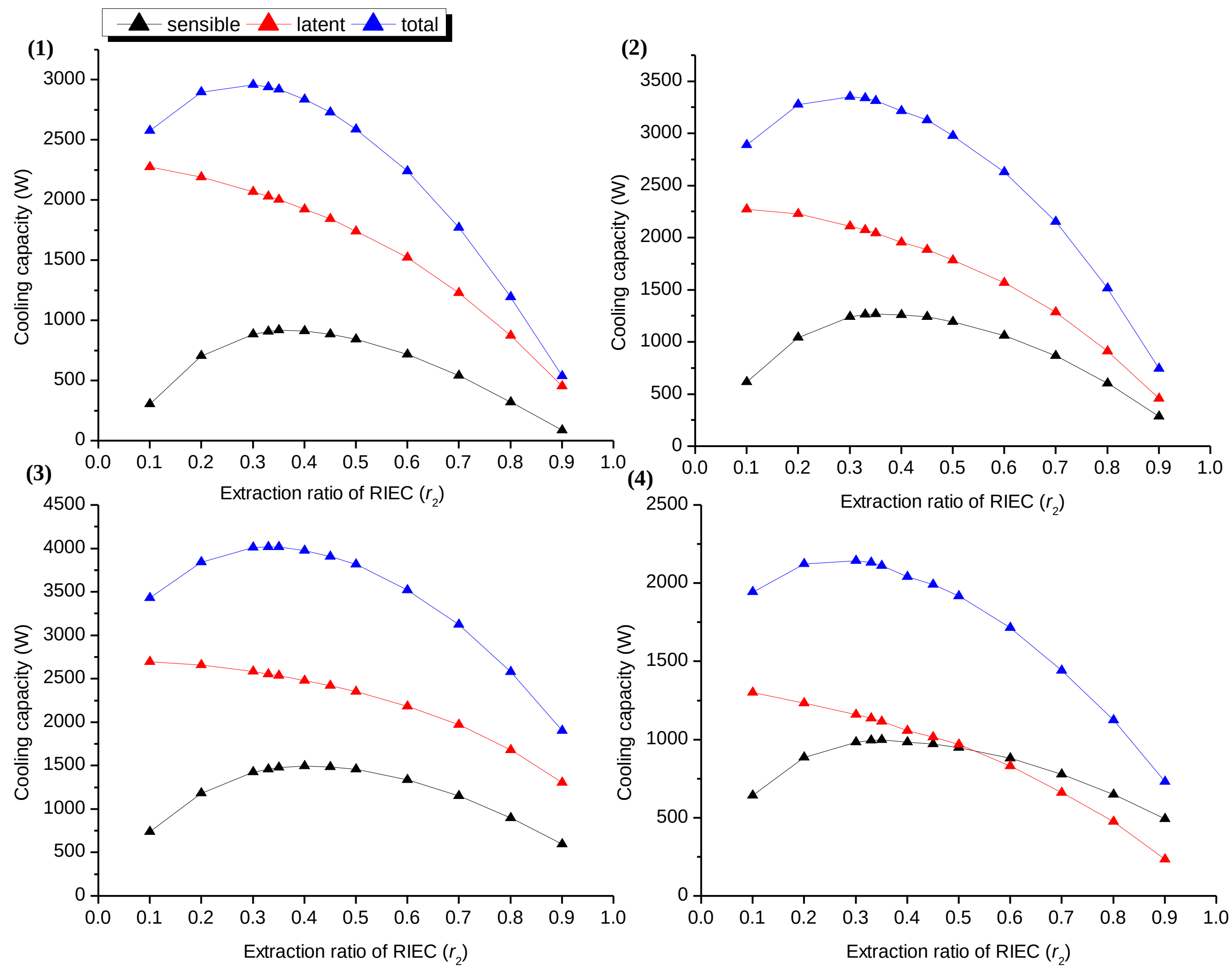

Case	Inlet air temperature (°C)	Inlet air humidity (g/kg)	Solar radiation (W/m2)
1	30	20	400
2	35	20	400
3	30	15	400
4	30	20	200

Fig.8 Cooling capacity under different extraction ratio of RIEC

The extraction ratio of RIEC in solar assisted LDD-RIEC system is optimized under fixed supply air rate. The total cooling capacity consisted of the latent cooling capacity (C_{lat}) and sensible cooling capacity (C_{sen}) is used as the optimization objective. Four cases with different air conditions and solar radiation were selected for optimization. The cooling capacities of LDD-RIEC system under various extraction ratios are shown in Fig.8. It can be seen that the trend of sensible, latent and total cooling capacity are similar under four cases. The latent cooling capacity keeps decreasing with the extraction ratio increases, while the sensible cooling capacity increases at the beginning and then decreases when the extraction ratio is larger than 0.35. Larger extraction ratio will bring larger inlet air flow rate to LDD in order to enable a fixed supply air rate. Both the moisture removal rate and outlet air temperature of LDD decrease if more air is handled by a certain LDD. The former weakens the cooling performance of RIEC in the next stage significantly as the evaporative cooling process greatly depends on the inlet air humidity. However, the higher extraction ratio enhances RIEC cooling performance. Overall, the maximum cooling capacity is achieved when the extraction ratio is about 0.3. Thus, the optimal extraction air ratio of RIEC is 0.3 considering the interacted influence of dehumidifier, regenerator, RIEC and solar collector.

4.3 Influence of solar collector area

The solar collector area has great influences on the solution concentration and solution temperature which thereby affect solution regeneration rate and moisture removal rate. In this section, the influence of solar collector area is discussed by analyzing solution parameters, air parameters and system cooling performance.

Fig.9 shows the influence of solar collector area on moisture removal rate. It can be seen that the moisture removal rate of LDD increases from 0 to 12.5 g/kg with the solar collector area increases from 0 to 80 m^2. More thermal energy is collected by larger solar collector which therefore results in higher inlet solution temperature. As the regeneration rate significantly improves with the increase of inlet solution temperature [39], the outlet solution concertation of regenerator or inlet solution concertation of dehumidifier increases. The moisture removal rate is therefore improved. However, the solubility of LiCl is limited. Under normal cases, LiCl would precipitate from the liquid solution and cause pipe clogged when solution mass fraction is higher than 45%, which results in unsustainable operation of the system. Therefore the moisture removal rate keeps almost steady when the solar collector is larger than 50 m^2.

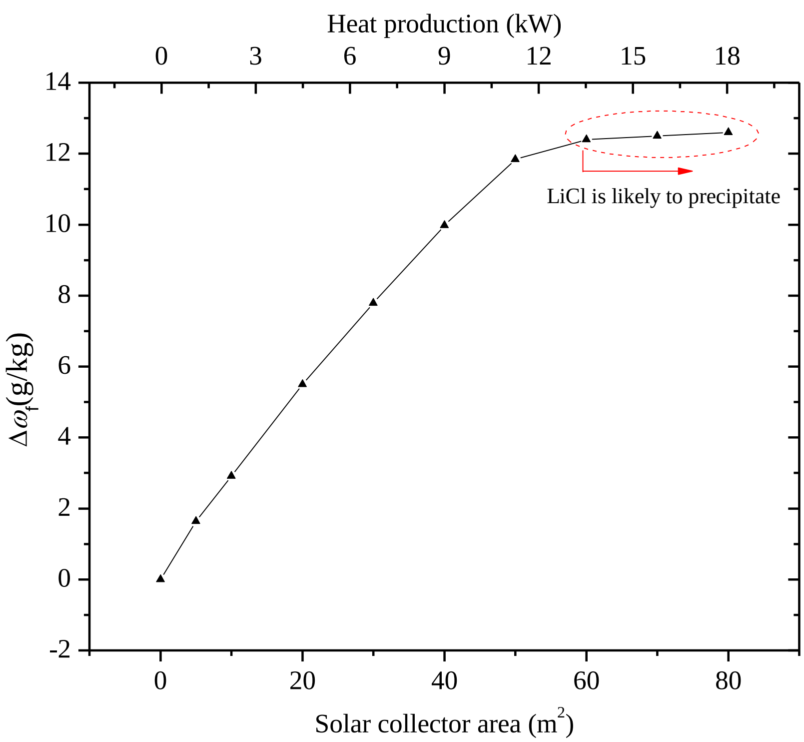

Fig.9 Influence of solar collector area on moisture removal rate

The detailed solution parameters and air parameters of LDD-RIEC system under different solar collector area are shown in Fig.10. The variation of solution concentration, inlet solution temperature of dehumidifier and inlet solution temperature of regenerator are shown in Fig.10(a). It can be seen that the solution mass fraction increases dramatically from 18.8% to 44.8% when the solar collector area increases from 5m^2 to 50m^2. Accordingly, the inlet solution temperature increases from 28.6℃ to 38.9℃ for dehumidifier and from 32.5℃ to 75.8℃ for regenerator. The high solution concentration benefits the dehumidification performance but the high inlet solution temperature worsens the dehumidification performance. However, in general, the solution mass fraction plays the dominate role because the cooling tower slows down the rising trend of inlet solution temperature of dehumidifier.

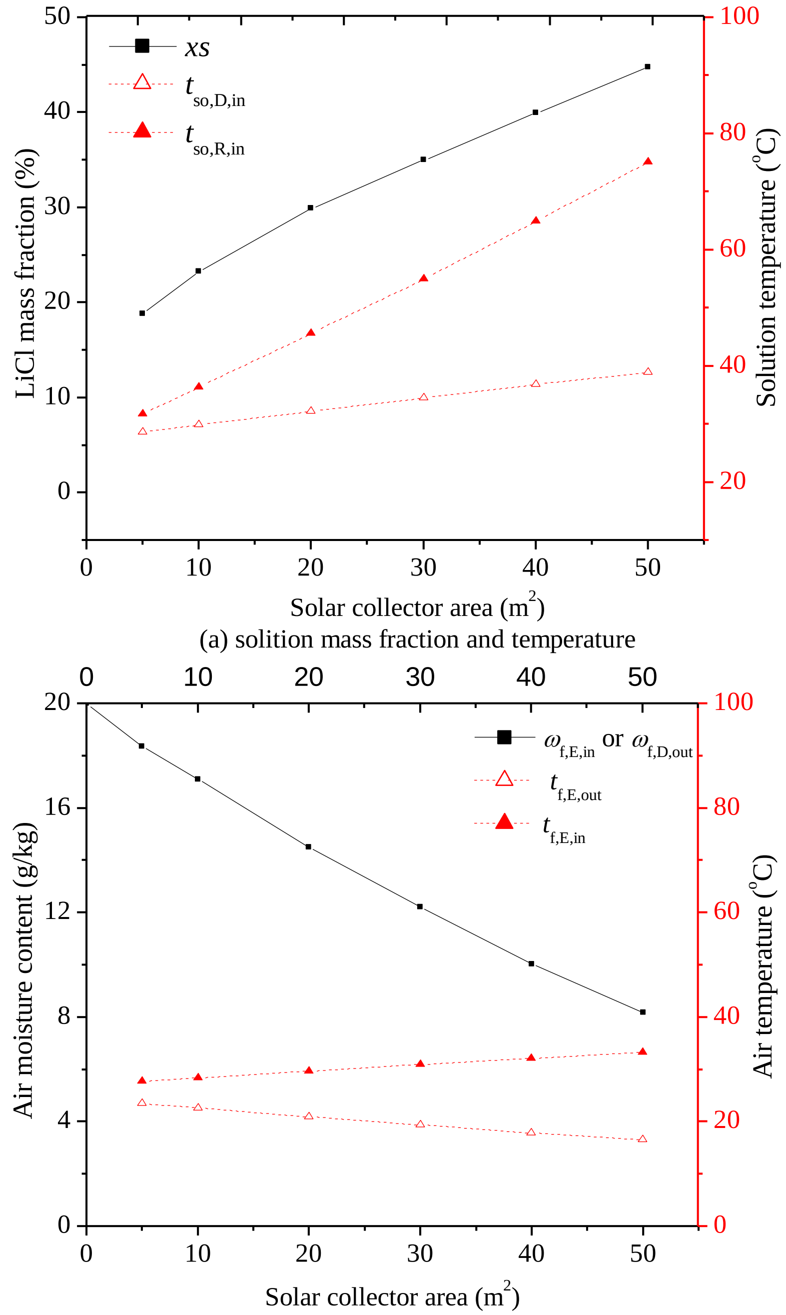

(a) solition mass fraction and temperature

(b) air moisture content and temperature

Fig.10 Influence of solar collector area on (a) solution conditions and (b) air conditions

The variation of outlet air humidity of dehumidifier, inlet air temperature of RIEC and outlet air temperature of RIEC are shown in Fig.10(b). It can be seen that the outlet air humidity of dehumidifier decreases while the temperature increases with the increase of solar collector area. The low air humidity enhances the water evaporation process in RIEC significantly and produces cooler supply air [40], but the higher inlet air temperature leads to warmer supply air. Thus, there is contradictory by adding solar collector area. However, it is noted that the outlet air temperature of RIEC keeps decreasing even though hotter inlet air is supplied at larger collector area. In sum, the inlet air humidity is the dominate parameter for RIEC performance considering the coupling effect of dehumidifier, regenerator and RIEC.

In the LDD-RIEC semi-centralized A/C system, fresh air handled by LDD-RIEC system takes part of responsibility for indoor cooling load. The influence of solar collector area on cooling capacity (C_{sen}, C_{lat}) and load removed rate (Q_{sen}, Q_{lat}) of LDD-RIEC system is analyzed as follows. The sensible and latent cooling capacity under different solar collector area are shown in Fig.11(a). Both the C_{sen} and C_{lat} increase significantly with increase of solar collector area. Based on the recommendation by ASHRAE handbook, the indoor air conditions should be within the psychrometric chart depict comfort zone, which ranges from 22℃ to 27℃ and 40% to 60% RH [41]. Accordingly, the ranges of load removed rate under different solar collector area are plotted in Fig.11(b). The negative value means the supply air temperature or humidity is higher than the comfort air conditions. Both the internal and fresh air cooling load will be handled by FCU. In this case, the LDD-RIEC actually acts as a fresh air pre-cooling system. It can be seen from Fig.11(b) that the fresh air takes no responsibility for cooling load until the solar collector area increases to 30m^2. In sum, in terms of thermal performance alone under fixed conditions, larger solar collector area enables better system performance by providing larger cooling capacity and load removed rate under the premise of no desiccant solution precipitation.

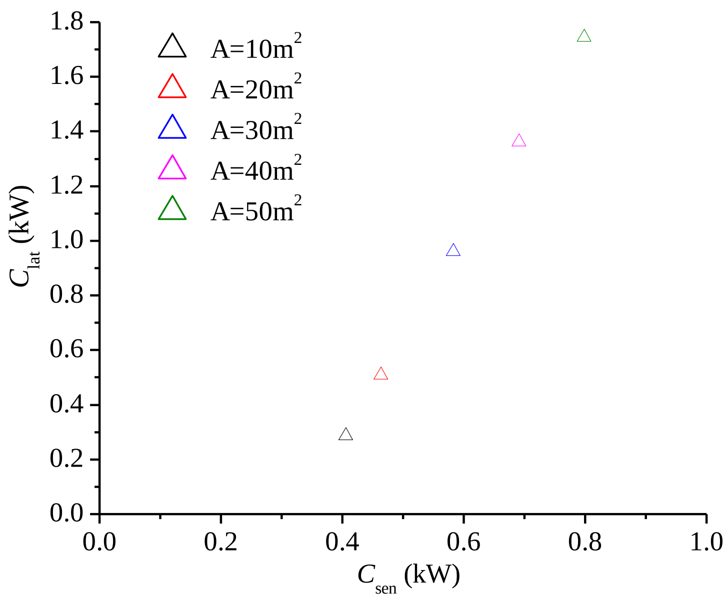

(a) influence of solar collector area on cooling capacity

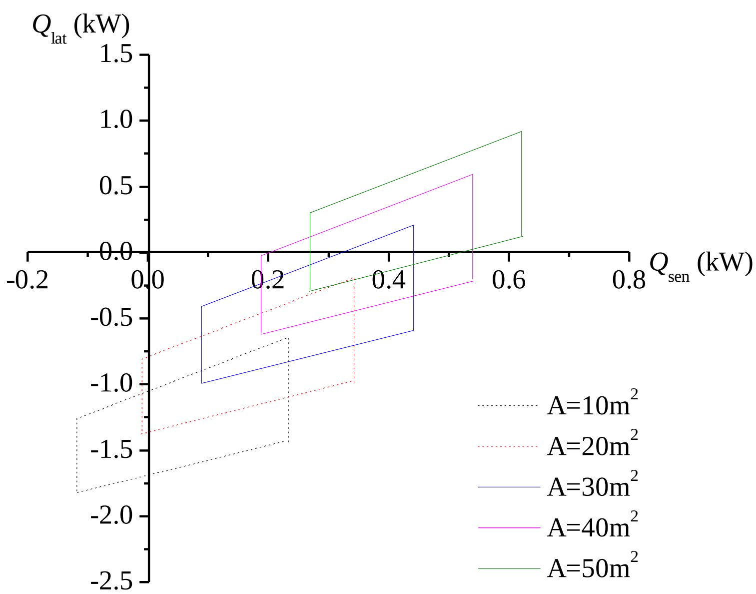

(b) influence of solar collector area on cooling load removed rate

Fig.11 Influence of solar collector area on (a) cooling capacity and (b) load removed rate

4.4 Influence of inlet air condition

The influences of inlet air temperature and humidity on cooling capacity and load removed rate of LDD-RIEC system are analyzed. Fig.12 shows the cooling capacity of LDD-RIEC system under different level of thermal energy collected by the solar collector (Q_{sc}) and inlet air condition ($t_{f,D,in}$, $\omega_{f,D,in}$). It can be seen that the thermal energy input plays dominate role in system cooling performance. Under the condition of fixed thermal energy input, the sensible cooling capacity increases dramatically with the increase of inlet air temperature, while the latent cooling capacity remains relatively steady. It is mainly because the outlet air temperature of RIEC is much less influenced by inlet air temperature owing to the pre-treatment process of LDD and HE4. Thus, the sensible cooling capacity of the system is larger at higher inlet air temperature. As shown in Fig.12(b), the sensible cooling capacity increases while latent cooling capacity decreases with the decrease of inlet air humidity. It is because the cooling efficiency of RIEC improves significantly but the dehumidification efficiency of LDD decreases at lower inlet air humidity [42,43].

In sum, the inlet air temperature has great effect on sensible cooling capacity of LDD-RIEC system but has little effect on its latent cooling capacity, while the inlet air humidity has large effect on both of the cooling capacity.

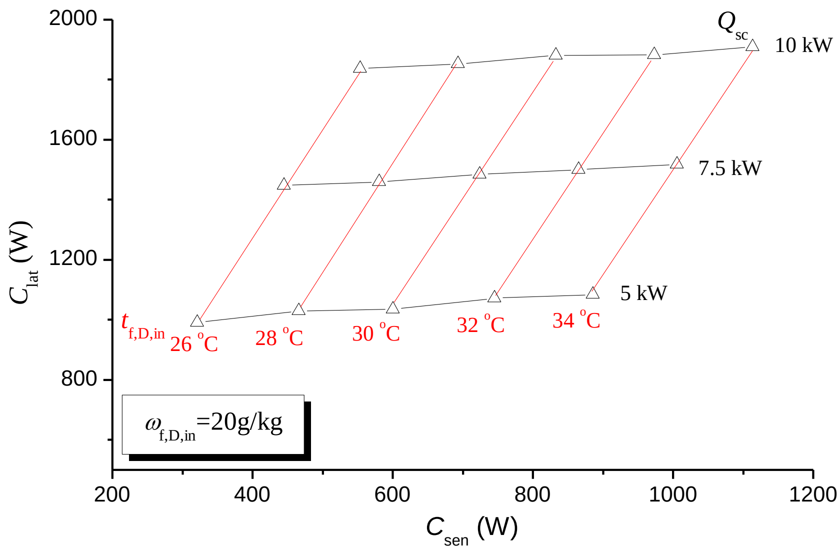

(a) Influence of inlet air temperature on cooling capacity of LDD-RIEC

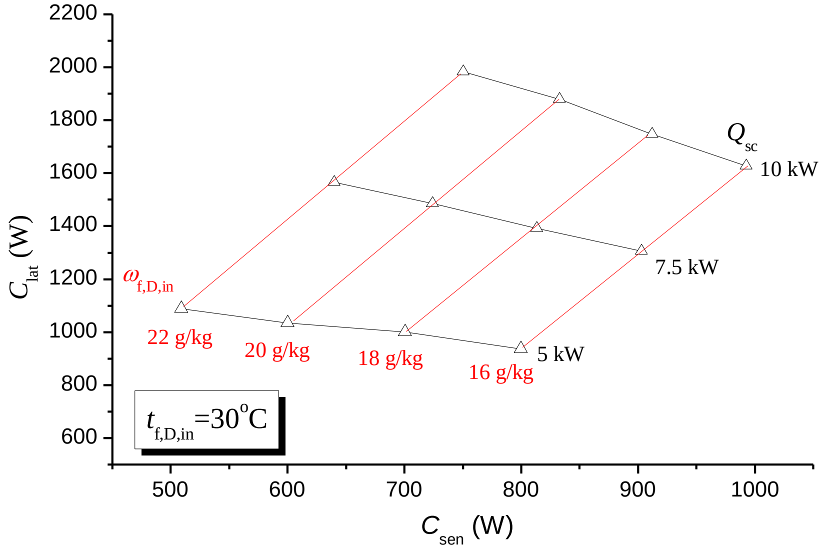

(b) Influence of inlet air humidity on cooling capacity of LDD-RIEC

Fig.12 Influence of inlet air condition on cooling capacity of LDD-RIEC system

Fig.13 shows the influence of inlet air condition on load removed rate by fresh air. It is found that the sensible load removed rate varies only within 4.3% ~5.5% when inlet air temperature increases by 8°C under fixed input thermal energy. The latent load removed rate variation is larger but also within 20%. It means that the supply air temperature and humidity are relatively steady under fluctuation of inlet air temperature. However, it can be noticed from Fig.13(b) that inlet air humidity has great influence on both the sensible and latent load removed rate. In sum, the inlet air temperature has limited effect on both the sensible and latent load removed rate of LDD-RIEC system, while the inlet air humidity has significant effect.

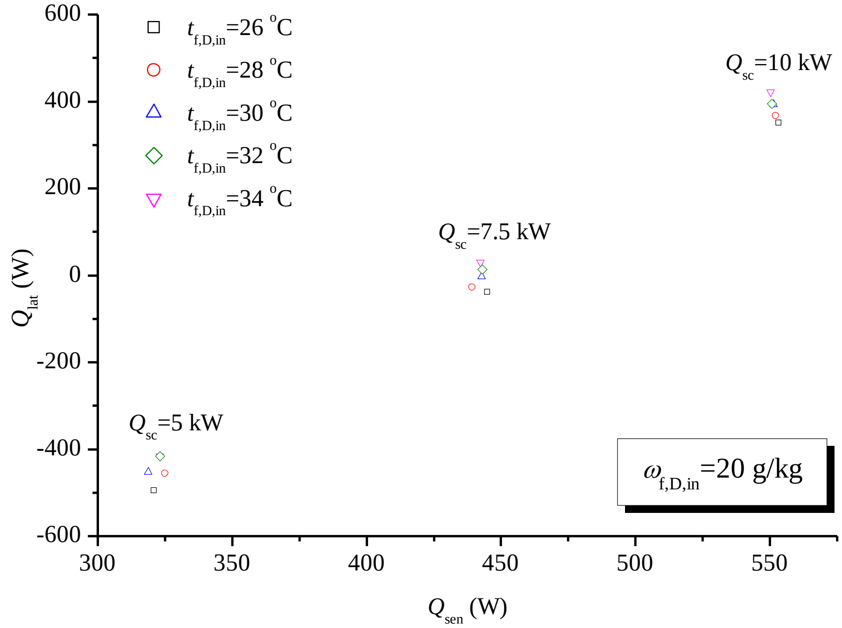

(a) Influence of inlet air temperature on load removed rate by fresh air

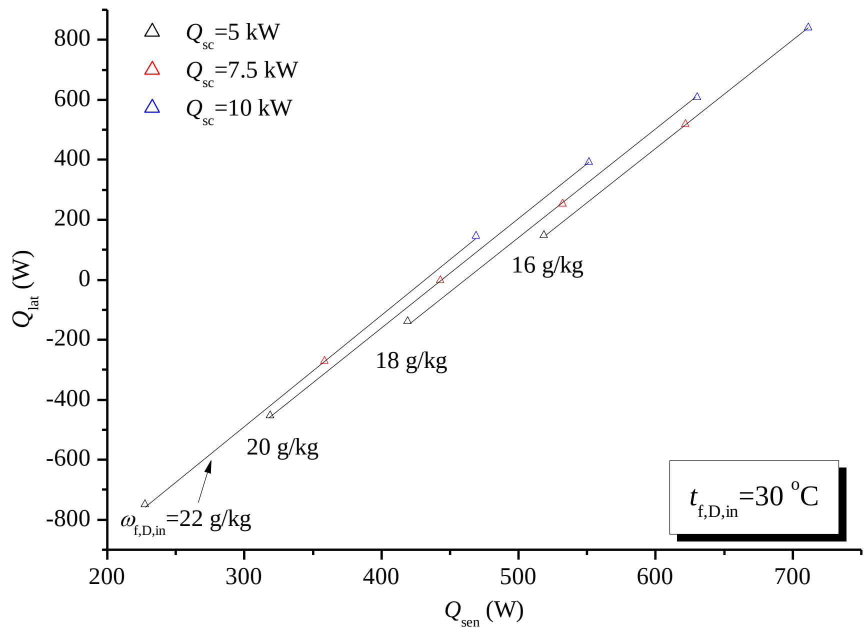

(b) Influence of inlet air humidity on load removed rate by fresh air

Fig.13 Influence of inlet air condition on load removed rate by fresh air

4.5 Energy saving potential and COP

The energy saving potential of LDD-RIEC semi-centralized A/C system is quantitatively evaluated with respect to the conventional MVCR system. Besides, the overall system's COP is investigated under various weather conditions. A detailed case is used for simulation. There are four people working (light work, typing) in an office of 20m^2. Each person is equipped with a computer with color monitor (230W/person). The cooling load density of lighting is 13W/m^2. The overall heat transfer coefficient of the envelope is supposed to be 2.4W/m^2·℃ and the envelope area is 27m^2. The fresh air flow rate is 0.07kg/s.

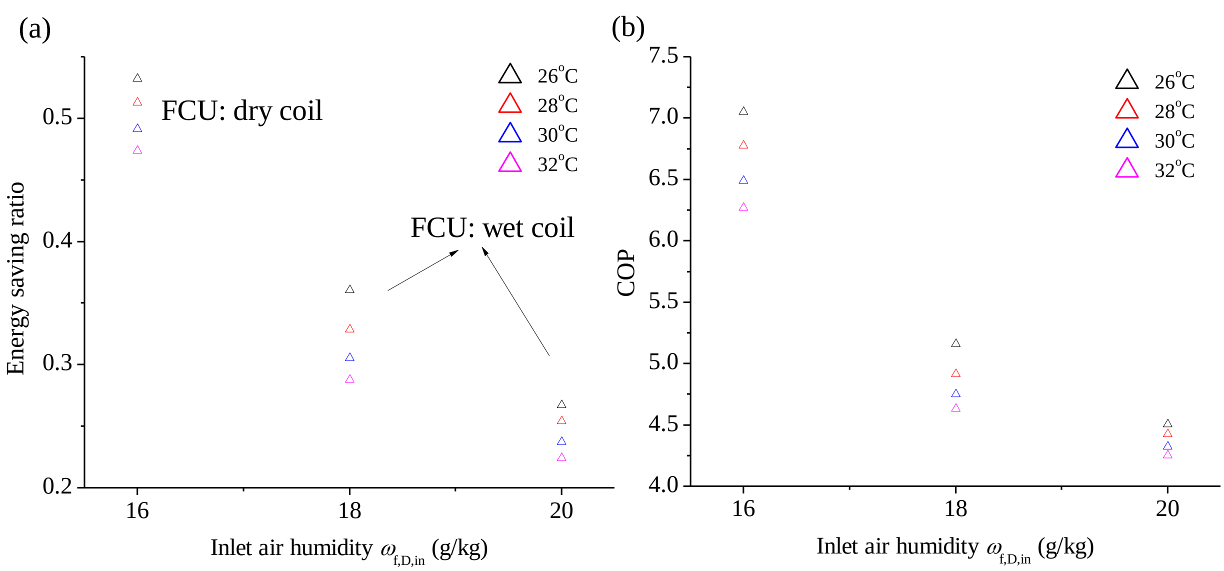

Temperature (oC)	Humidity (g/kg)	Fresh air load (W)	Internal load (W)	Total sensible load (W)	Total latent load (W)
26	16	595	1780	1480	895
26	18	945	1780	1480	1245
26	20	1295	1780	1480	1595
28	16	736	1912	1753	895
28	18	1086	1912	1753	1245
28	20	1436	1912	1753	1595
30	16	876	2044	2025	895
30	18	1226	2044	2025	1245
30	20	1576	2044	2025	1595
32	16	1017	2176	2298	895
32	18	1367	2176	2298	1245
32	20	1717	2176	2298	1595

Fig.14 (a) Energy saving ratio and (b) system's COP under different air conditions

The simulation results of energy saving ratio and COP under different air conditions are shown in Fig.14. The cooling load under each condition is listed out in the table. The energy saving ratio and COP are attractive with a range from 22.4% to 53.2% and 4.3 to 7.1, respectively. It can be seen that the energy saving ratio is higher at low inlet air humidity. It can be explained as follows. The total latent load is smaller under low fresh air humidity so that the latent load can be fully covered by treated fresh air. The FCU is able to operate under dry-coil condition, which largely improves the chiller's efficiency by producing high temperature chilled water. With the increase of inlet air humidity, the treated fresh air is unable to handle all latent load, so the FCU operates at wet-coil condition to deal with the rest of sensible and latent load. It can be also noticed that the energy saving ratio of low air temperature is slightly higher than that of high temperature at fixed air humidity. It is because more sensible load can be removed by treated fresh air. The system COP shows the same trend with energy saving potential.

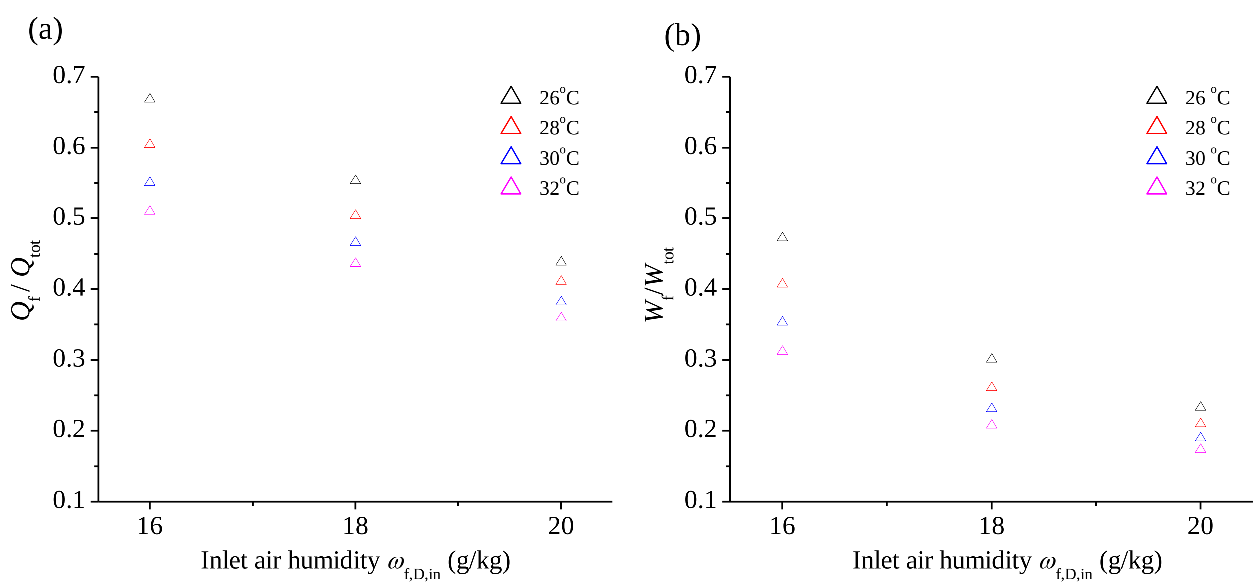

Fig.15 (a) load removed ratio by fresh air and (b) energy consumption ratio for treating fresh air

Fig.15 shows the load removed ratio by fresh air and energy consumption ratio for treating fresh air under various inlet air conditions. The load removed ratio is higher at low air humidity and temperature. The treated fresh air can handle as much as 67% cooling load when the fresh air is 26℃ and 16g/kg. Under all the conditions, the energy consumption ratio for treating fresh air is much smaller than the load removed ratio by fresh air, which proves the LDD-RIEC is an energy-effective approach for fresh air treatment.

The FCU operating condition (dry-coil or wet-coil) will affect the system performance because it decides the chiller's COP. The energy saving ratio and system's COP under different fresh air ratio and chiller's COP are shown in Fig.16. It can be seen that the system's COP and energy saving ratio increases with the increase of chiller's COP and fresh air ratio. The maximum energy saving ratio is 56.5% and system COP is 7.6 when the fresh air ratio (r_1) is 70% and chiller's COP is 4.62 (FCU operates under dry-coil condition). However, 30% energy saving can be still achieved when the fresh air ratio (r_1) is 30% and chiller's COP is 3.3 (FCU operates under wet-coil condition). In sum, energy efficiency of the system is higher when FCU operates at dry-coil condition. Thus, it is an optimal design that all latent load can be handle by the treated fresh air.

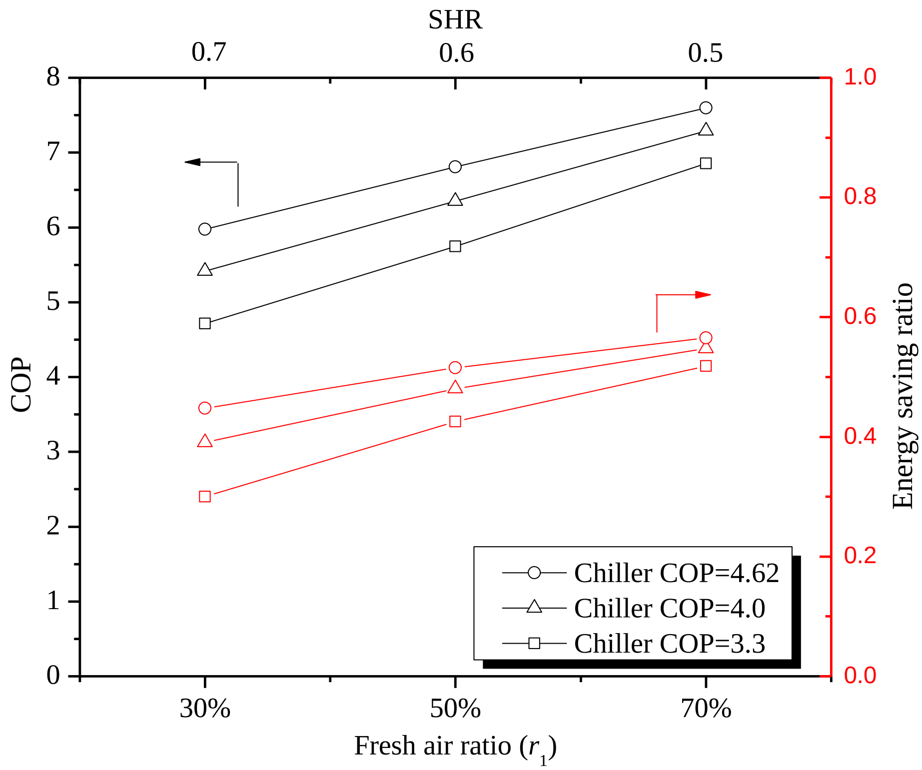

Fig.16 Influence of fresh air ratio and chiller's COP

5. Conclusion

The solar assisted liquid desiccant dehumidifier and regenerative indirect evaporative cooling (LDD-RIEC) semi-centralized air-conditioning (A/C) system was investigated in this paper. The system model was developed by solving the heat and mass transfer equations of each component integrally in a closed loop. The main results are as follows.

1. The proposed system can provide supply air of 17.2℃ and 9.8g/kg when ambient air is 30℃ and 20g/kg.
2. The optimal extraction air ratio of RIEC is 0.3 considering the interacted influence of dehumidifier, regenerator and RIEC.

3. In terms of thermal performance alone under fixed operating conditions, larger solar collector area can improve both the moisture removal rate and cooling capacity of the LDD-RIEC system. However, the capacity will reach the peak when the solar collector area increases to a certain value because of the limited solubility of desiccant.
4. Inlet air temperature has great effect on sensible cooling capacity of LDD-RIEC system but has little effect on its latent cooling capacity, while the air humidity has large effect on both of the cooling capacity. Inlet air temperature has limited effect on the sensible and latent load removed rate of LDD-RIEC system, while the inlet air humidity has significant effect.
5. The energy saving ratio and COP of LDD-RIEC semi-centralized A/C system are attractive, ranging from 22.4% to 53.2% and 4.3 to 7.1, respectively, under various inlet air temperature (26℃~32℃) and humidity (16g/kg~20g/kg).
6. The energy efficiency of LDD-RIEC semi-centralized A/C system is higher when FCU operates at dry-coil condition. Thus, it is an optimal design that all latent load can be handled by the treated fresh air.

Acknowledgement

This research is financially supported by the Research Institute of Sustainable Urban Development of The Hong Kong Polytechnic University and the Housing Authority of the Hong Kong SAR Government with account No. K-ZJK1.

References

[1] Pérez-Lombard, L., Ortiz, J., & Pout, C. (2008). A review on buildings energy consumption information. Energy and buildings, 40(3), 394-398.

[2] D. Yogi Goswami, Yuwen Zhao. (2007). Proceedings of ISES world congress 2007 (Vol.1 – Vol.5) : solar energy and human settlement. Springer.

[3] Kuo, N. W., Chiang, H. C., & Chiang, C. M. (2008). Development and application of an integrated indoor air quality audit to an international hotel building in Taiwan. Environmental monitoring and assessment, 147(1-3), 139-147.

[4] Alahmer, A. (2016). Thermal analysis of a direct evaporative cooling system enhancement with desiccant dehumidification for vehicular air conditioning. Applied Thermal Engineering, 98, 1273-1285.

[5] Mohammad, A. T., Mat, S. B., Sulaiman, M. Y., Sopian, K., & Al-Abidi, A. A. (2013). Survey of hybrid liquid desiccant air conditioning systems. Renewable and Sustainable Energy Reviews, 20, 186-200.

[6] Gao, W. Z., Cheng, Y. P., Jiang, A. G., Liu, T., & Anderson, K. (2015). Experimental investigation on integrated liquid desiccant–Indirect evaporative air cooling system utilizing the Maisotesenko–Cycle. Applied Thermal Engineering, 88, 288-296.

[7] Jain, S., Dhar, P. L., & Kaushik, S. C. (1995). Evaluation of solid-desiccant-based evaporative cooling cycles for typical hot and humid climates. International journal of Refrigeration, 18(5), 287-296.

[8] Mavroudaki, P., Beggs, C. B., Sleigh, P. A., & Halliday, S. P. (2002). The potential for solar powered single-stage desiccant cooling in southern Europe. Applied Thermal Engineering, 22(10), 1129-1140.

[9] Halliday, S. P., Beggs, C. B., & Sleigh, P. A. (2002). The use of solar desiccant cooling in the UK: a feasibility study. Applied Thermal Engineering, 22(12), 1327-1338.

[10] Qi, R., & Lu, L. (2014). Energy consumption and optimization of internally cooled/heated liquid desiccant air-conditioning system: A case study in Hong Kong. Energy, 73, 801-808.

[11] Xuan, Y. M., & Xiao, F. (2009). Analysis of energy efficiency of a hybrid liquid desiccant and evaporative cooling system in Hong Kong. Building Science, 25(2), 84-89.

[12] Finocchiaro, P., Beccali, M., & Nocke, B. (2012). Advanced solar assisted desiccant and evaporative cooling system equipped with wet heat exchangers. Solar Energy, 86(1), 608-618.

[13] La, D., Dai, Y. J., Li, Y., Tang, Z. Y., Ge, T. S., & Wang, R. Z. (2013). An experimental investigation on the integration of two-stage dehumidification and regenerative evaporative cooling. Applied energy, 102, 1218-1228.

[14] Mohammad, A. T., Mat, S. B., Sulaiman, M. Y., Sopian, K., & Al-abidi, A. A. (2013). Historical review of liquid desiccant evaporation cooling technology. Energy and Buildings, 67, 22-33.

[15] Watt, J. R., & Brown, W. K. (1997). Evaporative air conditioning handbook-3rd edition. Fairmont Press: 1997.

[16] Li, Y., Lu, L., & Yang, H. (2010). Energy and economic performance analysis of an open cycle solar desiccant dehumidification air-conditioning system for application in Hong Kong. Solar Energy, 84(12), 2085-2095.

[17] Qi, R., Lu, L., & Huang, Y. (2014). Energy performance of solar-assisted liquid desiccant air-conditioning system for commercial building in main climate zones. Energy conversion and Management, 88, 749-757.

[18] La, D., Dai, Y. J., Li, Y., Tang, Z. Y., Ge, T. S., & Wang, R. Z. (2013). An experimental investigation on the integration of two-stage dehumidification and regenerative evaporative cooling. Applied energy, 102, 1218-1228.

[19] Enteria, N., Yoshino, H., Takaki, R., Mochida, A., Satake, A., & Yoshie, R. (2013). Effect of regeneration temperatures in the exergetic performances of the developed desiccant-evaporative air-conditioning system. International journal of refrigeration, 36(8), 2323-2342.

[20] El Hourani, M., Ghali, K., & Ghaddar, N. (2014). Effective desiccant dehumidification system with two-stage evaporative cooling for hot and humid climates. Energy and Buildings, 68, 329-338.

[21] Woods, J., & Kozubal, E. (2013). A desiccant-enhanced evaporative air conditioner: numerical model and experiments. Energy Conversion and Management, 65, 208-220.

[22] Sohani, A., Sayyaadi, H., Balyani, H. H., & Hoseinpoori, S. (2016). A novel approach using predictive models for performance analysis of desiccant enhanced evaporative cooling systems. Applied Thermal Engineering, 107, 227-252.

[23] Kim, M. H., Park, J. S., & Jeong, J. W. (2013). Energy saving potential of liquid desiccant in evaporative-cooling-assisted 100% outdoor air system. Energy, 59, 726-736.

[24] Goldsworthy, M., & White, S. (2011). Optimisation of a desiccant cooling system design with indirect evaporative cooler. International Journal of refrigeration, 34(1), 148-158.

[25] Zhang, F., Yin, Y., & Zhang, X. (2017). Performance analysis of a novel liquid desiccant evaporative cooling fresh air conditioning system with solution recirculation. Building and Environment, 117, 218-229.

[26] Lee, J., & Lee, D. Y. (2013). Experimental study of a counter flow regenerative evaporative cooler with finned channels. International Journal of Heat and Mass Transfer, 65, 173-179.

[27] Hasan, A. (2012). Going below the wet-bulb temperature by indirect evaporative cooling: analysis using a modified ε-NTU method. Applied Energy, 89(1), 237-245.

[28] Riangvilaikul, B., & Kumar, S. (2010). Numerical study of a novel dew point evaporative cooling system. Energy and Buildings, 42(11), 2241-2250.

[29] Duan, Z., Zhan, C., Zhang, X., Mustafa, M., Zhao, X., Alimohammadisagvand, B., & Hasan, A. (2012). Indirect evaporative cooling: Past, present and future potentials. Renewable and Sustainable Energy Reviews, 16(9), 6823-6850.

[30] Yutong, L., & Hongxing, Y. (2008). Investigation on solar desiccant dehumidification process for energy conservation of central air-conditioning systems. Applied Thermal Engineering, 28(10), 1118-1126.

[31] Conde, M. R. (2004). Properties of aqueous solutions of lithium and calcium chlorides: formulations for use in air conditioning equipment design. International Journal of Thermal Sciences, 43(4), 367-382.

[32] Y.A Cengel, Heat and Mass Transfer: A Practical Approach, McGraw-Hill Companies, Inc., Singapore, 2006.

[33] Riangvilaikul, B., & Kumar, S. (2010). Numerical study of a novel dew point evaporative cooling system. Energy and Buildings, 42(11), 2241-2250.

[34] Chen, Y., Luo, Y., & Yang, H. (2015). A simplified analytical model for indirect evaporative cooling considering condensation from fresh air: development and application. Energy and Buildings, 108, 387-400.

[35] Li, Y., Lu, L., & Yang, H. (2010). Energy and economic performance analysis of an open cycle solar desiccant dehumidification air-conditioning system for application in Hong Kong. Solar Energy, 84(12), 2085-2095.

[36] Walker, A., Mahjouri, F., & Stiteler, R. (2004). Evacuated-tube heat-pipe solar collectors applied to the recirculation loop in a federal building. In Proceeding of solar 2004 conference.

[37] Riangvilaikul, B., & Kumar, S. (2010). Numerical study of a novel dew point evaporative cooling system. Energy and Buildings, 42(11), 2241-2250.

[38] Q. Ge, J. Liu, X. Chen, Z. Fang. (2009). A study on the mass transfer coefficient in counter flow dehumidifier. Chinese Society of Refrigeration Society 2009 Annual Meeting, Sichuang, China.

[39] Yin, Y., & Zhang, X. (2010). Comparative study on internally heated and adiabatic regenerators in liquid desiccant air conditioning system. Building and Environment, 45(8), 1799-1807.

[40] Zhao, X., Li, J. M., & Riffat, S. B. (2008). Numerical study of a novel counter-flow heat and mass exchanger for dew point evaporative cooling. Applied Thermal Engineering, 28(14), 1942-1951.

[41] Handbook, A. S. H. R. A. E. (2001). Fundamentals. American Society of Heating, Refrigerating and Air Conditioning Engineers, Atlanta, 111.

[42] Zhan, C., Zhao, X., Smith, S., & Riffat, S. B. (2011). Numerical study of a M-cycle cross-flow heat exchanger for indirect evaporative cooling. Building and Environment, 46(3), 657-668.

[43] Wang, L., Xiao, F., Zhang, X., & Kumar, R. (2016). An experimental study on the dehumidification performance of a counter flow liquid desiccant dehumidifier. International Journal of Refrigeration, 70, 289-301.